Dynamics of a two-atom Raman coupled model interacting with two quantized cavity fields

Christopher C. Gerry
Department of Physics, St. Bonaventure University, St. Bonaventure, New York 14778

H. Huang
Department of Physics and Astronomy, University of Rochester, Rochester, New York 14627
(Received 19 August 1991)

We describe the quantum dynamics of a two-atom Raman coupled model interacting with two quantized cavity electromagnetic fields as an extension of the previously discussed single-atom Raman coupled model [C. C. Gerry and J. H. Eberly, Phys. Rev. A **42**, 6805 (1990)]. In particular we study the atomic-population dynamics and the dynamics of the photon statistics in the two cavity modes. We present evidence of cooperative effects.

PACS number(s): 42.50.Hz, 42.50.Dv, 42.50.Fx

I. INTRODUCTION

Recently, the quantum dynamics of a single-atom Raman coupled to two quantized cavity fields was discussed [1]. The model consists of a three-level atom in the Λ configuration where the excited state is taken to be far off resonance with any cavity mode (see Fig. 1). The dynamics of this system displayed interesting behavior, rather different generally than obtained in the usual Jaynes-Cummings model of a two-level atom interacting with a single quantized cavity [2]. For example, assuming coherent states for both modes the atomic inversion between the two nondegenerate ground states exhibits periodic revivals but with many secondary revivals as well. These secondary revivals become less significant for higher average photon numbers. The collapse and revival patterns were partially explained in Ref. [1] but have been more fully explained, at least for the case of equal average photon numbers in both modes, by Cardimona *et al.* [3]. It was also shown in Ref. [1] that the Raman coupled model can produce nonclassical photon states exhibiting antibunching, violations of the Cauchy-Schwartz inequality, and squeezing.

It has been shown [4] for the case of many two-level atoms interacting with a single-mode field that cooperative behavior between the atoms (i.e., as in the Dicke model [5]) can enhance some nonclassical effects such as squeezing. Similar results have been shown for multiphoton generalizations of the Dicke model [6]. It seems natural then to investigate the possibility of cooperative behavior in a many-atom Raman model. In this paper we do just that by considering a two-atom Raman coupled model interacting with the two quantized cavity fields. This model, like the one-atom case, is exactly solvable. Previously, many authors have studied the dynamics of the interaction between two two-level atoms and a single cavity field [7] and cooperative effects have been noted.

This paper is organized as follows. In Sec. II we present the model, describing the relevant Dicke-type atomic states. The dynamics of the system is obtained by solving the time-dependent Schrödinger equation. In Sec. III we study the population dynamics of the two-atom system. In Sec. IV we examine the photon statistics, and in Sec. V we conclude the paper with a brief summary. However, before proceeding to the next section we should point out that much of our graphical work, particularly in Sec. IV, will be compared to similar work in Ref. [1], and the reader should consult that paper to make detailed comparison.

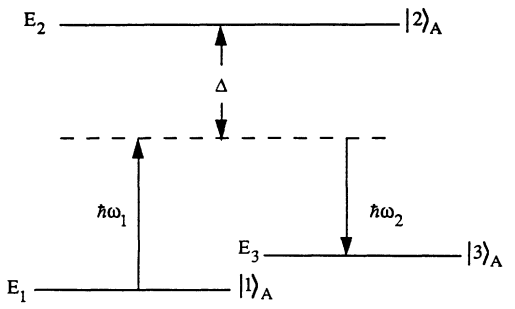

FIG. 1. Energy-level diagram of a single-atom Raman coupled model. The detuning Δ is assumed to be large.

II. MODEL HAMILTONIAN AND DYNAMICS

We first review the single-atom Raman coupled model of Ref. [1]. The three-level single-atom atomic states are labeled $|1\rangle_A$, $|2\rangle_A$, and $|3\rangle_A$, with energies E_1, E_2, and E_3, respectively, and are arranged as in Fig. 1. States $|1\rangle_A$ and $|3\rangle_A$ are the ground states, and $|2\rangle_A$ is the excited state which is assumed to be far off resonance with either of the cavity modes. Cavity mode 1 has frequency ω_1, while mode 2 has ω_2. We assume the cavity is tuned consistent with two-photon energy conservation ($E_3-E_1=\hbar\omega_1-\hbar\omega_2$) so that there is only one detuning parameter Δ, defined as

$$\hbar\Delta=E_2-E_1-\hbar\omega_1=E_2-E_3-\hbar\omega_2 . \tag{2.1}$$

We assume $\hbar\Delta$ to be large ($\hbar\Delta \gg E_3-E_1$) so that state

$|2\rangle_A$ may be adiabatically eliminated, effectively rendering the system a two-level atom. The effective Hamiltonian for this system (apart from additive constants) is [1]

$$H_{(1\text{ atom})}=H_0+H_{I,\text{eff}}\ , \tag{2.2}$$

where

$$H_0=\frac{\hbar}{2}\omega_0\sigma_0+\hbar\omega_1 a_1^\dagger a_1+\hbar\omega_2 a_2^\dagger a_2 \tag{2.3a}$$

and

$$H_{I,\text{eff}}=-\hbar\lambda(\sigma_+ a_1 a_2^\dagger+\sigma_- a_1^\dagger a_2)\ . \tag{2.3b}$$

Here a_1 ($a_1^\dagger$) and a_2 ($a_2^\dagger$) are the boson annihilation (creation) operators of the cavity modes, σ_+ and σ_- are the effective raising and lowering operators between atomic levels 1 and 3, σ_0 is the difference of the occupation number operators between levels 3 and 1, and λ is the effective coupling constant, and $\hbar\omega_0=E_3-E_1=\hbar(\omega_1-\omega_2)$. The number states for the field modes are $|n_1,n_2\rangle_F=|n_1\rangle_{F1}\otimes|n_2\rangle_{F2}$, just the direct product of number states for modes 1 and 2.

The many-atom case is easily constructed just as for the usual Dicke model [7]. We define the collective atomic operators

$$J_0=\tfrac{1}{2}\sum_{i=1}^{N}\sigma_0^{(i)},\quad J_\pm=\sum_{i=1}^{N}\sigma_\pm^{(i)}\ , \tag{2.4}$$

where N is the number of atoms and the $\sigma^{(i)}$ are the atomic operators for the ith atom. The operators $J_0, J_\pm$ satisfy the angular momentum algebra. The Hamiltonian for the N-atom case then is

$$H_{(N\text{-atom})}=\hbar\omega_0 J_0+\hbar\omega_1 a_1^\dagger a_1+\hbar\omega_2 a_2^\dagger a_2 -\lambda\hbar(J_+ a_1 a_2^\dagger+J_- a_1^\dagger a_2)\ . \tag{2.5}$$

In what follows, we consider only the special case when $N=2$.

For the two-atom case, the possible two-atom states are

$$\begin{aligned}|1,1\rangle_A&=|1\rangle_{A_1}\otimes|1\rangle_{A_2}\ ,\\ |1,3\rangle_A&=|1\rangle_{A_1}\otimes|3\rangle_{A_2}\ ,\\ |3,1\rangle_A&=|3\rangle_{A_1}\otimes|1\rangle_{A_2}\ ,\\ |3,3\rangle_A&=|3\rangle_{A_1}\otimes|3\rangle_{A_2}\ ,\end{aligned} \tag{2.6}$$

where A_1 and A_2 refer to atoms 1 and 2. It is convenient to introduce the Dicke states $|j,m\rangle_D$, which for the two-atom system we have $j=1$, $m=1,0,-1$. The Dicke states are related to the two-atom states above according to

$$\begin{aligned}|1,-1\rangle_D&=|1,1\rangle_A\ ,\\ |1,0\rangle_D&=\frac{1}{\sqrt{2}}(|1,3\rangle_A+|3,1\rangle_A)\ ,\\ |1,-1\rangle_D&=|3,3\rangle_A\ .\end{aligned} \tag{2.7}$$

If we assume that initially both atoms are in the ground state with n_1 photons in mode 1 and n_2 in mode 2, then at $t=0$

$$\begin{aligned}|\psi(0)\rangle_{n_1n_2}&=|1,1\rangle_A|n_1,n_2\rangle_F\\ &=|1,-1\rangle_D|n_1n_2\rangle_F\ .\end{aligned} \tag{2.8}$$

On the other hand, if we assume both modes are initially in coherent states, then at $t=0$ we have

$$|\psi(0)\rangle_{\alpha_1\alpha_2}=|1,-1\rangle_D\sum_{n_1=0}^{\infty}\sum_{n_2=0}^{\infty}C_{n_1}(\alpha_1)C_{n_2}(\alpha_2)|n_1,n_2\rangle_F\ , \tag{2.9}$$

where

$$C_{n_i}(\alpha_i)=\exp(-|\alpha_i|^2/2)\frac{\alpha_i^{n_i}}{\sqrt{n_i!}},\quad i=1,2 \tag{2.10}$$

The average photon number in the ith mode is $\bar{n}_i=|\alpha_i|^2$. Now the interaction Hamiltonian connects the state $|1,1\rangle_A|n_1,n_2\rangle_F$ to the states

$$|3,3\rangle_A|n_1-2,n_2+2\rangle_F\ ,$$

$$|3,1\rangle_A|n_1-1,n_2+1\rangle_F\ ,$$

and

$$|1,3\rangle_A|n_1-1,n_2+1\rangle_F\ .$$

These states are eigenstate of the free Hamiltonian

$$H_0=\hbar\omega_0 J_0+\hbar\omega_1 a_1^\dagger a_1+\hbar\omega_2 a_2^\dagger a_2 \tag{2.11}$$

with energy eigenvalues

$$E_{n_1n_2}=\hbar[\omega_1(n_1-1)+\omega_2(n_2+1)]\ . \tag{2.12}$$

For times $t>0$ we write the state vector as

$$|\psi(t)\rangle=\sum_{n_1,n_2=0}^{\infty}\exp(-iE_{n_1n_2}t/\hbar)C_{n_1}(\alpha_1)C_{n_2}(\alpha_2)[A_{(1,1)}^{(n_1,n_2)}(t)|1,1\rangle_A|n_1n_2\rangle_F+A_{(3,3)}^{(n_1,n_2)}|3,3\rangle_A|n_1-2,n_2+2\rangle_F +A_{(1,3)}^{(n_1,n_2)}(t)(|1,3\rangle_A+|3,1\rangle_A)|n_1-1,n_2+1\rangle_F] \tag{2.13}$$

or in terms of the Dicke states of Eq. (2.7)

$$|\psi(t)\rangle=\sum_{n_1,n_2=0}^{\infty}\exp(-iE_{n_1n_2}t/\hbar)C_{n_1}(\alpha_1)C_{n_2}(\alpha_2) \times[A_-^{(n_1,n_2)}(t)|1,-1\rangle_D|n_1,n_2\rangle_F+A_+^{(n_1,n_2)}(t)|1,+1\rangle_D|n_1-2,n_2+2\rangle_F +\sqrt{2}A_0^{(n_1,n_2)}(t)|1,0\rangle_D|n_1-1,n_2+1\rangle_F]\ , \tag{2.14}$$

where the relabeling of the A coefficients from Eqs. (2.13) and (2.14) is obvious. The time-dependent Schrödinger equation leads to the following equations for the A coefficients:

$$i\dot{A}_{-}^{(n_1,n_2)}=-2\lambda\sqrt{n_1(n_2+1)}\,A_0^{(n_1,n_2)}\ , \tag{2.15a}$$

$$i\dot{A}_{+}^{(n_1,n_2)}=-2\lambda\sqrt{(n_1-1)(n_2+1)}\,A_0^{(n_1,n_2)}\ , \tag{2.15b}$$

$$i\dot{A}_0^{(n_1,n_2)}=-\lambda[\sqrt{n_1(n_2+1)}\,A_{-}^{(n_1,n_2)}+\sqrt{(n_1-1)(n_2+2)}\,A_{+}^{(n_1,n_2)}] \tag{2.15c}$$

with the initial conditions

$$A_{-}^{(n_1,n_2)}(0)=1,\quad A_{+}^{(n_1,n_2)}(0)=A_0^{(n_1,n_2)}(0)=0\ . \tag{2.16}$$

The solutions of these equations are easily solved, for example, by using Laplace transforms, to obtain

$$A_{-}^{(n_1,n_2)}(t)=1-\frac{2a_{n_1n_2}^2}{a_{n_1n_2}^2+b_{n_1n_2}^2}\times\sin^2[\sqrt{\tfrac{1}{2}(a_{n_1n_2}^2+b_{n_1n_2}^2)}\lambda t]\ , \tag{2.17a}$$

$$A_{+}^{(n_1,n_2)}(t)=-\frac{2a_{n_1n_2}b_{n_1n_2}}{a_{n_1n_2}^2+b_{n_1n_2}^2}\times\sin^2[\sqrt{\tfrac{1}{2}(a_{n_1n_2}^2+b_{n_1n_2}^2)}\lambda t]\ , \tag{2.17b}$$

and

$$A_0^{(n_1,n_2)}(t)=-i\frac{a_{n_1n_2}}{\sqrt{2(a_{n_1n_2}^2+b_{n_1n_2}^2)}}\times\sin[\sqrt{2(a_{n_1n_2}^2+b_{n_1n_2}^2)}\lambda t]\ , \tag{2.17c}$$

where

$$a_{n_1n_2}=\sqrt{n_1(n_2+1)}\ ,\qquad b_{n_1n_2}=\sqrt{(n_1-1)(n_2+2)}\ . \tag{2.18}$$

This concludes our discussion of the model and the solutions of the Schrödinger equation.

III. ATOMIC DYNAMICS

We now turn to the consideration of the atomic dynamics, in particular the time evolution of the atomic populations.

The complete atomic inversion for the two-atom system is given by

$$W(t)=\langle\Psi(t)|J_0|\Psi(t)\rangle=\sum_{n_1=0}^{\infty}P_{n_1}(\bar{n}_1)P_{n_2}(\bar{n}_2)[|A_{+}^{(n_1,n_2)}(t)|^2-|A_{-}^{(n_1,n_2)}(t)|^2]\ , \tag{3.1}$$

where

$$P_{n_i}(\bar{n}_1)=|C_{n_i}(\alpha_i)|^2=\exp(-\bar{n}_i)\frac{\bar{n}_i^{n_i}}{n_i!}\quad(i=1,2) \tag{3.2}$$

are the coherent-state photon probability distributions. It turns out to be more revealing of the dynamics to study the atomic level-occupation probabilities which are given as

$$\Pi_{11}(t)=\sum_{n_1=0}^{\infty}\sum_{n_2=0}^{\infty}P_{n_1}(\bar{n}_1)P_{n_2}(\bar{n}_2)|A_{-}^{(n_1,n_2)}(t)|^2$$
$$=\sum_{n_1=0}^{\infty}\sum_{n_2=0}^{\infty}P_{n_1}(\bar{n}_1)P_{n_2}(\bar{n}_2)\left[1-\frac{2a_{n_1n_2}^2}{(a_{n_1n_2}^2+b_{n_1n_2}^2)}[1-\cos(\Omega_{n_1n_2}t)]+\frac{a_{n_1n_2}^4}{(a_{n_1n_2}^2+b_{n_1n_2}^2)}[\tfrac{3}{2}-2\cos(\Omega_{n_1n_2}t)+\tfrac{1}{2}\cos(2\Omega_{n_1n_2}t)]\right]\ , \tag{3.3a}$$

$$\Pi_{33}(t)=\sum_{n_1=0}^{\infty}\sum_{n_2=0}^{\infty}P_{n_1}(\bar{n}_1)P_{n_2}(\bar{n}_2)|A_{+}^{(n_1,n_2)}(t)|^2$$
$$=\sum_{n_1=0}^{\infty}\sum_{n_2=0}^{\infty}P_{n_1}(\bar{n}_1)P_{n_2}(\bar{n}_2)\frac{(a_{n_1n_2}b_{n_1n_2})^2}{(a_{n_1n_2}^2+b_{n_1n_2}^2)^2}[\tfrac{3}{2}-2\cos(\Omega_{n_1n_2}t)+\tfrac{1}{2}\cos(2\Omega_{n_1n_2}t)]\ , \tag{3.3b}$$

$$\Pi_{13}(t)=2\sum_{n_1=0}^{\infty}\sum_{n_2=0}^{\infty}P_{n_1}(\bar{n}_1)P_{n_2}(\bar{n}_2)|A_0^{(n_1,n_2)}(t)|^2$$
$$=\tfrac{1}{2}\sum_{n_1=0}^{\infty}\sum_{n_2=0}^{\infty}P_{n_1}(\bar{n}_1)P_{n_2}(\bar{n}_2)\frac{a_{n_1n_2}^2}{(a_{n_1n_2}^2+b_{n_1n_2}^2)}[1-\cos(2\Omega_{n_1n_2}t)]\ , \tag{3.3c}$$

where Π_{11} and Π_{33} are the probabilities that both atoms are in states 1 and 3, respectively, while Π_{13} is the probability that one atom is in state 1, the other in state 3. Also in the above expressions

$$\Omega_{n_1 n_2}=\lambda\sqrt{2(a^2_{n_1 n_2}+b^2_{n_1 n_2})}$$
$$=\sqrt{2}\lambda(2n_1 n_2+3n_1-n_2-2)^{1/2} \tag{3.4}$$

are the two-atom Rabi frequencies. Obviously

$$\Pi_{11}(t)+\Pi_{33}(t)+\Pi_{13}(t)=1 \tag{3.5}$$

and, of course, the atomic inversion is

$$W(t)=\Pi_{33}(t)-\Pi_{11}(t)\ . \tag{3.6}$$

In what follows we concentrate on the quantities $\Pi_{33}(t)$ and $\Pi_{13}(t)$, since $\Pi_{11}(t)$ is dependent on these through Eq. (3.5). The subtraction in eq. (3.6) actually deletes some of the information on the secondary revivals.

We first consider the special case when $\bar{n}_2=0$. We obtain

$$\Pi_{33}(t)=\sum_{n_1=0}^{\infty}P_{n_1}(\bar{n}_1)\left[\frac{2n_1(n_1-1)}{3n_1-2}\right]^2$$
$$\times[\tfrac{3}{2}-2\cos(\Omega_{n_1 0}t)+\tfrac{1}{2}\cos(2\Omega_{n_1 0}t)]\ , \tag{3.7a}$$

$$\Pi_{13}(t)=\tfrac{1}{2}\sum_{n_1=0}^{\infty}P_{n_1}(\bar{n}_1)\left[\frac{n_1}{3n_1-2}\right][1-\cos(2\Omega_{n_1 0}t)]\ , \tag{3.7b}$$

where

$$\Omega_{n_1 0}=\lambda[2(3n_1-2)]^{1/2}\ . \tag{3.8}$$

The time evolutions of these quantities are shown in Fig. 2 for $\bar{n}_1=10$. In the quantity $\Pi_{33}(t)$, the largest amplitude is oscillating at frequency $\Omega_{n_1 0}$. We can use the usual arguments to predict the locations of the revivals [2b]. The time between revivals T_R can be estimated by finding the time when neighboring oscillators at $\bar{n}_1$ and $\bar{n}_1+1$ differ by a phase of 2π

$$[\Omega_{\bar{n}_1+1,0}-\Omega_{\bar{n}_1,0}]T_R=2\pi \tag{3.9}$$

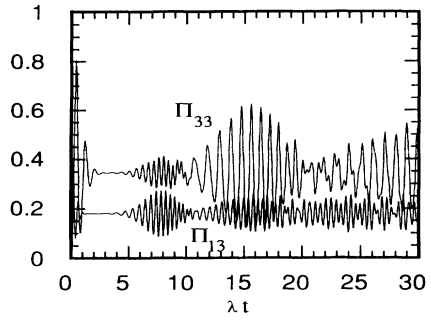

FIG. 2. $\Pi_{33}(t)$ and $\Pi_{13}(t)$ vs λt for $\bar{n}_1=10$, $\bar{n}_2=0$.

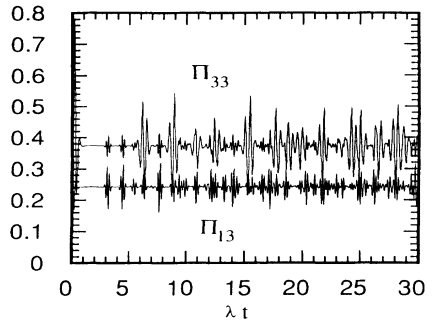

FIG. 3. Same as Fig. 2 but with $\bar{n}_1=10$, $\bar{n}_2=5$.

or

$$\lambda T_R\sqrt{2}(\sqrt{3\bar{n}_1+1}-\sqrt{3\bar{n}_1-2})=2\pi \tag{3.10}$$

from which we obtain, for $\bar{n}_1\gg 1$,

$$\lambda T_R\simeq 2\pi\left[\frac{2\bar{n}_1}{3}\right]^{1/2}\ . \tag{3.11}$$

For $\bar{n}_1=10$, we obtain $\lambda T_R\simeq 16$, which indeed is in the center of the large amplitude oscillation of $\Pi_{33}(t)$. The other terms in the series are oscillating at the frequencies $2\Omega_{n_1 0}$, so we would expect, by the same argument as above, a smaller amplitude revival at $(\lambda T_R/2)$, which is indeed present at $\lambda t\simeq 8$ for $\Pi_{33}(t)$. For $\Pi_{13}(t)$, on the other hand, only the frequencies $2\Omega_{n_1 0}$ contribute, and the first large revival occurs as expected at $\lambda t\simeq 8$. The revival patterns for $\bar{n}_2=0$ are similar to those seen for two two-level atoms interacting with a single cavity mode. See, for example, Deng and Iqbal *et al.* [7].

We now consider the case for $\bar{n}_1,\bar{n}_2\neq 0$. For example, in Fig. 3 we display the time records of $\Pi_{33}(t)$ and $\Pi_{13}(t)$ for $\bar{n}_1=10$, $\bar{n}_2=5$ and for $\bar{n}_1=30$, $\bar{n}_2=30$ in Fig. 4, and we note that the pattern of revivals is significantly different than the case when $\bar{n}_2=0$. (Such a distinction was also evident in the one-atom case [1]). Here we attempt an explanation of the revivals using the method adopted in Ref. [1].

Let us consider Eq. (3.3b) for $\Pi_{33}(t)$. This can be written as

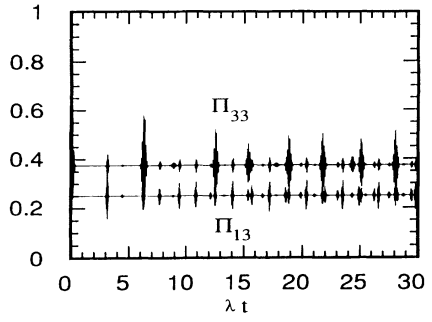

FIG. 4. Same as Fig. 2 but with $\bar{n}_1=\bar{n}_2=30$.

$$\Pi_{33}(t)=\mathrm{Re}\left[\sum_{n_1=0}^{\infty}\sum_{n_2=0}^{\infty}P_{n_1}(\bar{n}_1)P_{n_2}(\bar{n}_2)\frac{(a_{n_1n_2}b_{n_1n_2})^2}{(a_{n_1n_2}^2+b_{n_1n_2}^2)^2}\left[\tfrac{3}{2}-2\exp(i\Omega_{n_1n_2}t)+\tfrac{1}{2}\exp(2i\Omega_{n_1n_2}t)\right]\right]. \tag{3.12}$$

The rapid oscillations in the time records are from the dominant Rabi oscillations at $\Omega_{\bar{n}_1\bar{n}_2}=\sqrt{2}\lambda[2\bar{n}_1\bar{n}_2+3\bar{n}_1-\bar{n}_2-2)^{1/2}$. We now expand the frequencies $\Omega_{n_1n_2}$ in a Taylor series about $\bar{n}_1$ and $\bar{n}_2$ to obtain (to first order)

$$\Omega_{n_1n_2}=\Omega_{\bar{n}_1\bar{n}_2}+\frac{\lambda}{\sqrt{2}}\frac{2\bar{n}_2}{(2\bar{n}_1\bar{n}_2+3\bar{n}_1-\bar{n}_2-2)^{1/2}}(n_1-\bar{n}_1)+\frac{\lambda}{\sqrt{2}}\frac{2\bar{n}_1}{(2\bar{n}_1\bar{n}_2+3\bar{n}_1-\bar{n}_2-2)^{1/2}}(n_2-\bar{n}_2)+\cdots \tag{3.13}$$

Following the arguments of Ref. [1], for the terms oscillating at $\Omega_{n_1n_2}$, revivals occur at times T_R when

$$\frac{\lambda T_R}{\sqrt{2}}\frac{2\bar{n}_2+3}{(2\bar{n}_1\bar{n}_2+3\bar{n}_1-\bar{n}_2-2)^{1/2}}=2\pi k,\quad k=0,1,2,\ldots,$$
$$\frac{\lambda T_R}{\sqrt{2}}\frac{2\bar{n}_1-1}{(2\bar{n}_1\bar{n}_2+3\bar{n}_1-\bar{n}_2-2)^{1/2}}=2\pi l,\quad l=0,1,2,\ldots. \tag{3.14}$$

Multiplying these equations together we obtain

$$\frac{(\lambda T_R)^2}{2}\frac{(2\bar{n}_2+3)(2\bar{n}_1-1)}{(2\bar{n}_1\bar{n}_2+3\bar{n}_1-\bar{n}_2-2)}=4\pi^2kl\ . \tag{3.15}$$

Now for large $\bar{n}_1,\bar{n}_2$ we obtain $(\lambda T_R)^2=4\pi^2kl$ or

$$\lambda T_R=2\pi\sqrt{m}\ ,m=kl=0,1,2,\ldots. \tag{3.16}$$

Dividing the two Eqs. (3.14), for $\bar{n}_1,\bar{n}_2$ large gives

$$\frac{\bar{n}_2}{\bar{n}_1}=\frac{k}{l}\ . \tag{3.17}$$

Equation (3.16) predicts a sequence of revivals at $\lambda T_R=2\pi$, 8.89, 10.88, 4π, 14.05, etc., just as for the one-atom case in [1]. Primary revivals seem to occur at 2π, 4π, etc. with secondary revivals 8.89, 10.88, etc. These are clearly visible in Figs. 3 and 4. Additional revivals from the terms in Eq. (3.12) oscillating at $2\Omega_{n_1n_2}$ are evident. Using the method of the previous analysis, these revivals can be predicted to occur at

$$\lambda T_R=\pi\sqrt{m}\ ,\quad m=0,1,2,\ldots, \tag{3.18}$$

and indeed, revivals can be seen in Figs. 3 and 4 at $\lambda T_R=\pi$, 4.44, 5.44, etc. It is apparent that we do not always get revivals at these times but when a revival *does* occur it is at one of these times. Of course, we have not taken Eq. (3.17) into account so it appears that the occurrence of the revivals is not completely explained. (For the special case of $\bar{n}_1=\bar{n}_2$ in the one-atom Raman coupled model see the paper by Cardimona *et al.* [3]). As $\bar{n}_1$ and $\bar{n}_2$ are increased, only the revivals at 2π, 4π, etc. seem to survive. See Fig. 5 for $\bar{n}_1=\bar{n}_2=100$.

Finally, in closing this section we point out that a similar set of revival patterns would be expected for the two-atom two-photon system with interaction Hamilton of the form $J_+a_1a_2+\mathrm{H.c.}$ The one-atom version of this has been discussed by Gou [8].

IV. FIELD STATISTICS

In this section we examine certain aspects of the field statistics with an interest in obtaining evidence for cooperative effects. In particular, we examine the occurrence of photon antibunching in the modes, anticorrelations between the modes, and violations of the Cauchy-Schwartz inequality indicating a nonclassical correlation between the modes. To characterize the statistical properties of the radiation we use the same quantities as used in Ref. [1] which the reader may consult (and references therein).

In what follows, we shall need the quantities $\langle a_1^\dagger(t)a_1(t)\rangle,\langle a_2^\dagger(t)a_2(t)\rangle,\langle a_1^{\dagger2}(t)a_1^2(t)\rangle,\langle a_2^{\dagger2}(t)a_2^2(t)\rangle$, and $\langle a_1^\dagger(t)a_2^\dagger(t)a_2(t)a_1(t)\rangle$. These are given as

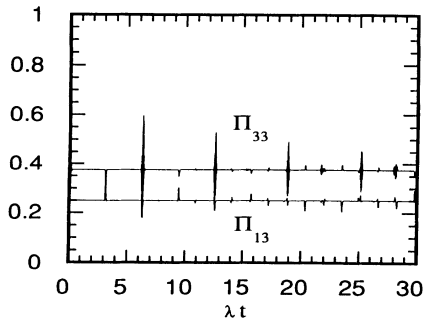

FIG. 5. Same as Fig. 2 but with $\bar{n}_1=\bar{n}_2=100$.

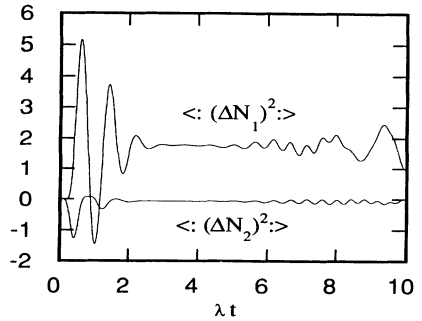

FIG. 6. $\langle:(\Delta N_1)^2:\rangle$ and $\langle:(\Delta N_2)^2:\rangle$ vs λt for $\bar{n}_1=10$, $\bar{n}_2=0$.

$$\langle a_1^\dagger(t)a_1(t)\rangle=\sum_{n_1=0}^{\infty}\sum_{n_2=0}^{\infty}n_1P_{n_1}(\bar{n}_1)P_{n_2}(\bar{n}_2)|A_-^{(n_1,n_2)}(t)|^2+\sum_{n_1=2}^{\infty}\sum_{n_2=0}^{\infty}(n_1-2)P_{n_1}(\bar{n}_1)P_{n_2}(\bar{n}_2)|A_+^{(n_1,n_2)}(t)|^2$$
$$+2\sum_{n_1=1}^{\infty}\sum_{n_2=0}^{\infty}(n_1-1)P_{n_1}(\bar{n}_1)P_{n_2}(\bar{n}_2)|A_0^{(n_1,n_2)}(t)|^2\,, \tag{4.1a}$$

$$\langle a_2^\dagger(t)a_2(t)\rangle=\sum_{n_1=0}^{\infty}\sum_{n_2=0}^{\infty}P_{n_1}(\bar{n}_1)P_{n_2}(\bar{n}_2)[n_2|A_-^{(n_1,n_2)}(t)|^2+(n_2+2)|A_+^{(n_1,n_2)}(t)|^2+2(n_2+1)|A_0^{(n_1,n_2)}(t)|^2]\,, \tag{4.1b}$$

$$\langle a_1^{\dagger 2}(t)a_1^2(t)\rangle=\sum_{n_1=1}^{\infty}\sum_{n_2=0}^{\infty}n_1(n_1-1)P_{n_1}(\bar{n}_1)P_{n_2}(\bar{n}_2)|A_-^{(n_1,n_2)}(t)|^2$$
$$+\sum_{n_1=3}^{\infty}\sum_{n_2=0}^{\infty}(n_1-2)(n_1-3)P_{n_1}(\bar{n}_1)P_{n_2}(\bar{n}_2)|A_+^{(n_1,n_2)}(t)|^2$$
$$+2\sum_{n_1=2}^{\infty}\sum_{n_2=0}^{\infty}(n_1-1)(n_2-2)|A_0^{(n_1,n_2)}(t)|^2\,, \tag{4.1c}$$

$$\langle a_2^{\dagger 2}(t)a_2^2(t)\rangle=\sum_{n_1=0}^{\infty}\sum_{n_2=0}^{\infty}P_{n_1}(\bar{n}_1)P_{n_2}(\bar{n}_2)[n_2(n_2-1)|A_-^{(n_1,n_2)}(t)|^2+(n_2+1)(n_2+2)|A_+^{(n_1,n_2)}(t)|^2$$
$$+2n_2(n_2+1)|A_0^{(n_1,n_2)}(t)|^2]\,, \tag{4.1d}$$

and

$$\langle a_1^\dagger(t)a_2^\dagger(t)a_2(t)a_1(t)\rangle=\sum_{n_1=0}^{\infty}\sum_{n_2=0}^{\infty}n_1n_2P_{n_1}(\bar{n}_1)P_{n_2}(\bar{n}_2)|A_-^{(n_1,n_2)}(t)|^2$$
$$+\sum_{n_1=2}^{\infty}\sum_{n_2=0}^{\infty}(n_1-2)(n_2+2)P_{n_1}(\bar{n}_1)P_{n_2}(\bar{n}_2)|A_+^{(n_1,n_2)}(t)|^2$$
$$+2\sum_{n_1=1}^{\infty}\sum_{n_2=0}^{\infty}(n_1-1)(n_2+1)P_{n_1}(\bar{n}_1)P_{n_2}(\bar{n}_2)|A_0^{(n_1,n_2)}(t)|^2\,. \tag{4.1e}$$

We first consider photon antibunching in the modes that may be characterized by the normally ordered variances of the number operators $N_i=a_i^\dagger a_i$

$$\langle:(\Delta N_i)^2:\rangle=\langle a_i^{\dagger 2}a_i^2\rangle-\langle a_i^\dagger a_i\rangle^2,\quad i=1,2\,. \tag{4.2}$$

Whenever $\langle:(\Delta N_i)^2:\rangle<0$, antibunched states exist. In Fig. 6 we plot $\langle:(\Delta N_i)^2:\rangle$ versus time (λt) for $\bar{n}_1=10$ and $\bar{n}_2=0$. Mode 2 apparently is always antibunched and indeed from Eqs. (4.1b) and (4.1d) for $\bar{n}_2=0$ it follows that

$$\langle:[\Delta N_2(t)]^2:\rangle=-\sum_{n_1=0}^{\infty}P_{n_1}(\bar{n}_1)|A_0^{(n_1 0)}(t)|^2\,, \tag{4.3}$$

which is always negative. In the transient regime the variances $\langle:(\Delta N_i)^2:\rangle$ do become more negative for both

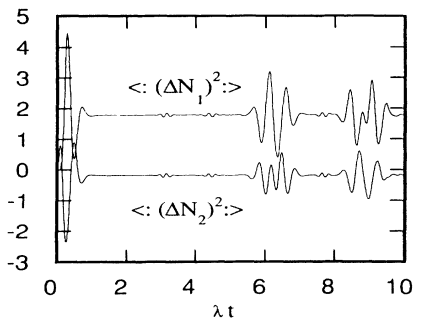

FIG. 7. Same as Fig. 6 but with $\bar{n}_1=10$, $\bar{n}_2=5$.

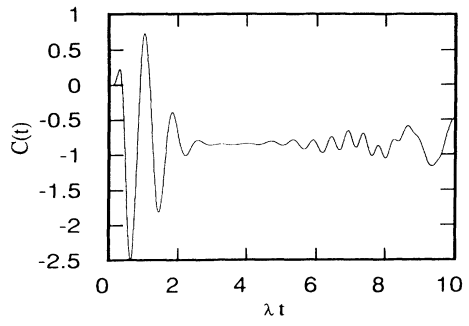

FIG. 8. $C(t)$ vs λt for $\bar{n}_1=10$, $\bar{n}_2=0$.

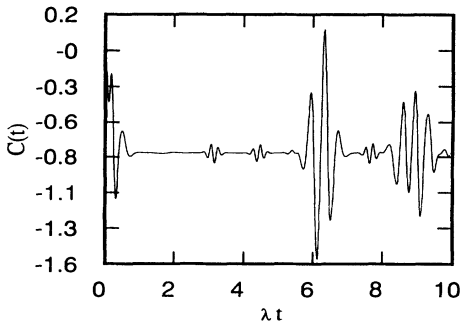

FIG. 9. Same as Fig. 8 but with $\bar{n}_1=10$, $\bar{n}_2=5$.

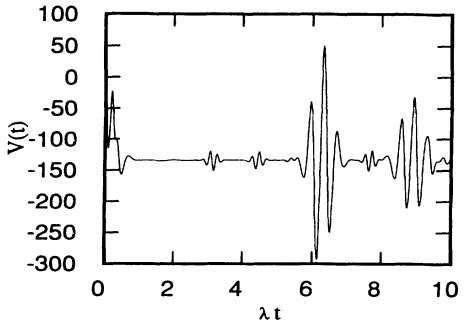

FIG. 11. Same as Fig. 10 but with $\bar{n}_1=10$, $\bar{n}_2=5$.

modes than for the one-atom case. (Compare with Fig. 6 of Ref. [1]). In Fig. 7 we plot these quantities for $\bar{n}_1=10$ and $\bar{n}_2=5$. Again we find, for mode 2, that the normally ordered variance is more negative than for the one-atom case while the fluctuations in mode 1 are more enhanced (see Fig. 7 of Ref. [1]). We thus see some evidence of cooperative behavior in the two-atom model in the production of photon antibunching.

Next we consider the cross-correlation function defined as

$$C(t)=\langle a_1^\dagger(t)a_2^\dagger(t)a_2(t)a_1(t)\rangle - \langle a_1^\dagger(t)a_1(t)\rangle\langle a_2^\dagger(t)a_2(t)\rangle \ , \tag{4.4}$$

which is proportional to the excess coincidence counting rate for a Hanbury Brown–Twiss-type experiment with two beams [9]. For $C=0$ the beams are uncorrelated, for $C>0$ they are correlated, and for $C<0$ they are anticorrelated. In Figs. 8 and 9 we present our results for $\bar{n}_1=10$ and $\bar{n}_2=0$ and $\bar{n}_1=10$ and $\bar{n}_2=5$, respectively. In the former case, comparing with Fig. 8(a) of Ref. [1], we see that $C(t)$ does indeed become more negative in the transient regime. The same is true for the second case in the transient regime and at the later time $\lambda t\simeq 2\pi$ [compare with Fig. 8(b) of Ref. [1]]. We thus obtain evidence of cooperative behavior in the production of anticorrelated light beams. Indeed from the form of the interaction, where a photon from one mode is destroyed while one is created in the other mode, we would expect the resulting light beams to be predominantly anticorrelated, and this appears to be reinforced in the two-atom case.

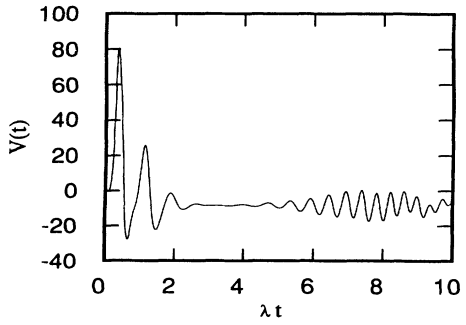

FIG. 10. $V(t)$ vs λt for $\bar{n}_1=10$, $\bar{n}_2=0$.

Finally, we consider the Cauchy-Schwartz inequality. We define the quantity

$$V(t)=\langle a_1^\dagger(t)a_2^\dagger(t)a_2(t)a_1(t)\rangle^2 - \langle a_1^{\dagger 2}(t)a_1^2(t)\rangle\langle a_2^{\dagger 2}(t)a_2^2(t)\rangle \ . \tag{4.5}$$

Whenever $V(t)>0$ the Cauchy-Schwartz inequality is violated indicating a nonclassical correlation between the beams. In Figs. 10 and 11 we display $V(t)$ for $\bar{n}_1=10$, $\bar{n}_2=0$ and $\bar{n}_1=10$, $\bar{n}_2=5$. Comparing these with Figs. 9(a) and 9(b) of Ref. [1] we see that for the case when $\bar{n}_1=10$, $\bar{n}_2=0$, the Cauchy-Schwartz inequality is slightly more violated than in the one-atom case at least in the transient regime, but at later times, unlike the one-atom case, is generally not violated. For $\bar{n}_1=10$ and $\bar{n}_2=5$ there is no initial transient violation as there is in the one-atom case, and the violation at $\lambda t\simeq 2\pi$ is less pronounced.

We close this section by noting that it would also be possible to consider the squeezing of the light beams in the modes. However, the form of the interaction Hamiltonian is not conducive to the efficient production of squeezed light, and indeed, in the one-atom case the amount of squeezing demonstrated was extremely small. We therefore do not pursue the squeezing in the present work.

V. SUMMARY AND DISCUSSION

In this paper we have discussed the quantum dynamics of two atoms that are Raman coupled to two quantized cavity fields. We have studied the dynamics of the atomic level populations and have shown the existence of distinct types of revivals in the time records of the Rabi oscillations. The locations of these revivals have been at least partially explained. Furthermore, we have examined some aspects of the photon statistics and have observed evidence of cooperative behavior in the production of antibunching in the modes and of anticorrelations between the modes. However, we find the Cauchy-Schwartz inequality less strongly violated in the two-atom case as compared to the one-atom case of Ref. [1], except for an initial transient with mode 2 in the vacuum.

It would perhaps be of interest to study the dynamics of the N-atom case. Previously the one- and two-photon Dicke models have been shown to produce cooperatively enhanced squeezing in a single-mode field [4,6]. The present model with N atoms has so far been studied only perturbatively for short times [10] where it has become clear that long-time solutions are required to observe any interesting behavior. Such long-time studies are currently under way and will be reported elsewhere.

ACKNOWLEDGMENT

The authors wish to thank Professor J. H. Eberly for discussions.

[1] C. C. Gerry and J. H. Eberly, Phys. Rev. A **42**, 6805 (1990).
[2] (a) E. T. Jaynes and F. W. Cummings, Proc. IEEE **51**, 89 (1963); for a review of developments since 1980 and many references, see (b) H.-I. Yoo and J. H. Eberly, Phys. Rep. **118**, 239 (1985).
[3] D. A. Cardimona, V. Kovanis, M. P. Sharma, and A. Gavrielides, Phys. Rev. A **43**, 3710 (1991).
[4] M. Butler and P. D. Drummond, Opt. Acta **33**, 1 (1986).
[5] R. H. Dicke, Phys. Rev. **93**, 99 (1954).
[6] C. C. Gerry and J. B. Togeas, Opt. Commun. **69**, 263 (1989).
[7] Z. Deng, Opt. Commun. **54**, 222 (1985); S. Mahmood and M. S. Zubairy, Phys. Rev. A **35**, 425 (1987); F. Lekien, E. P. Kadantseva, A. S. Schumovsky, Physica C **150**, 445 (1988); S. Mahmood, K. Zaheer, and M. S. Zubairy, Phys. Rev. A **37**, 1634 (1988); M. S. Iqbal, S. Mahmood, M. S. K. Razmi, and M. S. Zubairy, J. Opt. Soc. Am. B **5**, 1312 (1988); S. Mahmood and M. S. Zubairy, J. Mod. Opt. **37**, 243 (1990); M. A. Mir, T. Nasreen, and M. S. K. Razmi, Phys. Rev. A **41**, 4087 (1990).
[8] S.-C. Gou, Phys. Rev. A **40**, 5116 (1989).
[9] R. Loudon, Rep. Prog. Phys. **43**, 58 (1979).
[10] C. C. Gerry and J. B. Togeas (unpublished).